

# Numerical modeling of BP 1150 boiler by commercial numerical code<sup>☆</sup>

Bartłomiej Hernik\*

Institute of Power Engineering and Turbomachinery, Silesian University of Technology  
20 Konarskiego Street, 44-100 Gliwice, Poland

## Abstract

In this paper a numerical model was created for the combustion chamber of BP 1150 boilers of Opole Power Plant with an additional set of protection air system nozzles. The calculation was using Ansys Fluent CFD. Three cases of air distribution to OFA and SOFA nozzles were modeled. The ratio of air was increased to OFA and SOFA nozzles by taking secondary air from burners to decrease  $\text{NO}_x$  emission. The distribution of primary and secondary air was done so that the ratio of air from the protection air system was at a stable 10% of secondary air. A numerical simulation of the furnace of BP 1150 boilers confirmed that staggered air decreases  $\text{NO}_x$  emission and showed the  $\text{NO}_x$  concentrations at various levels of the combustion chamber.

Keywords: fossil fuels, numerical modeling, coal fired boiler

## 1. Introduction

Low emission fuel combustion in power plants, meaning limited  $\text{NO}_x$  emissions, has been developed worldwide since the early 1970s. In Poland the issue arose in the early 1990s when the first regulations appeared in this field. Now Poland is subject to the European Large Combustion Plant Directive, which imposes emission requirements. The Polish emission regulations [1] transpose the said Directive [2] providing for limits for  $\text{NO}_x$  emissions as set out in Table 1.

It is possible to obtain considerably lower emissions by using relatively cheap primary methods based on modification of the combustion process.

In this article a numerical model of the combustion chamber of BP 1150 boiler is presented. The numerical simulation was done using Ansys Fluent. One set of work of the protection air system (PAS) and three cases of distribution of air to OFA and SOFA nozzles was simulated. The ratio of air to OFA and SOFA nozzles was increased at the cost of secondary air from burners in order to decrease  $\text{NO}_x$  emission. The distribution of primary and secondary air was done so that the ratio of protection air remained at a stable 10% of secondary air. The numerical simulation of the working of the boiler's combustion chamber confirmed that increasing the air supply, after burning, to the OFA and SOFA nozzles at the cost of secondary air to the burners (staggered air), efficiently decreased  $\text{NO}_x$  emission.

<sup>☆</sup>Paper presented at the 10<sup>th</sup> International Conference on Research & Development in Power Engineering 2011, Warsaw, Poland

\*Corresponding author

Email address: bartlomiej.hernik@polsl.pl  
(Bartłomiej Hernik\*)

Table 1: Standard of NO<sub>x</sub> emission in  $\frac{mg}{m^3}$  converted into NO<sub>2</sub> by 6% O<sub>2</sub> on flue gas (bituminous coal combustion)

Nominal thermal power of source	Sources entering use pre 29.03.1990			Sources entering use post 28.03.1990	
	to 31.12.2007	from 01.01.2008 to 31.12.2015	till 01.01.2016	to 31.12.2015	till 01.01.2016
> 50 ≤ 500	600	600	600	500	500
> 500	540	500	200	500	200

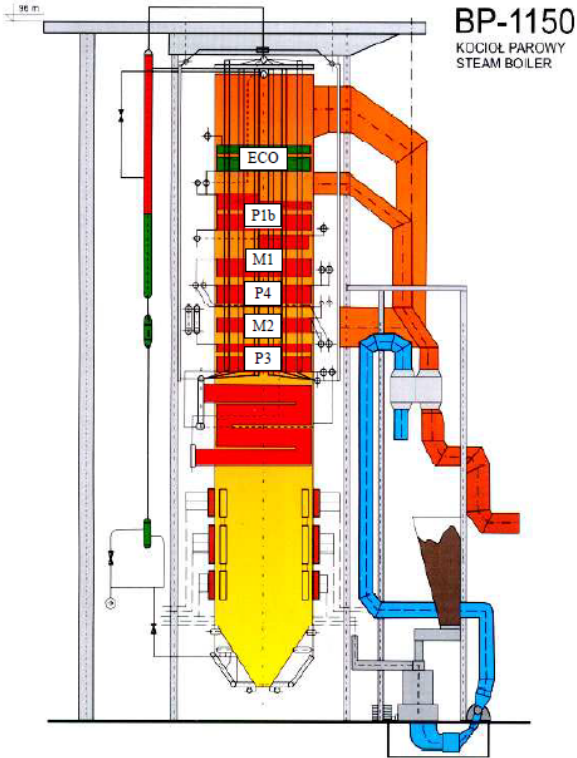


Figure 1: Scheme of BP 1150 boiler

## 2. Boilers specification

The BP 1150 boiler is a once-through boiler – Fig. 1, and a cross-section of the combustion chamber has the following dimensions: 14.3 m×15.7 m.

Jet burners was located in the corners of furnace between levels 18.2 m and 31.4 m and could be raked in the range  $\pm 20^\circ$ . The system of preparation of fuel for boilers number one and two is equipped in a five bowl RP-1043x milling system. Two burner nozzles in each corner are supplied by one mill. The burner nozzles in the bottom section are supplied by mill MW-1 and 2; in the middle section the burners are supplied by mills

MW-3 and 4; in the upper section the supply burners are supplied by mill number MW-5. The set of burners belonging to one set of mill have three secondary nozzles (bottom, middle and upper). The OFAs nozzles are located in the corners above the powdered fuel burners and on the front and rear wall at the level of 34.5 m; two SOFA nozzles are located on each wall. The SOFA nozzles was made as lifted in horizontal level and can be angled at  $45^\circ$ .

## 3. Model description with boundary conditions

Table 2: Basic info about case B of PAS

Outflow direction	The number of supplied nozzles	F, m <sup>2</sup>	w, $\frac{m}{s}$
L (left)	192	0.00234	33.87
C (central)	192	0.00255	31.08
P (right)	192	0.00234	33.87

The calculation was made with a coefficient of air excess  $\lambda_k''$  at the outlet of the combustion chamber equal to 1.15. Optimization of the protection air system by selecting the best number and configuring the protection air nozzle was investigated in order to supply the appropriate oxygen concentration in the boundary layer of flue gas, as presented in [3]. Optimizing PAS took into account the velocity and direction of the air at the end of the nozzles. The results of numerical simulations of working case B of PAS is presented below. Case B provided the most effective protection for the wall of the furnace against low

NO<sub>x</sub> corrosion (the smallest portion of CO in the boundary layer of flue gas). For this case only the nozzles located in the middle column of the four walls were used. Three directions of outflow were used, see Table 2.

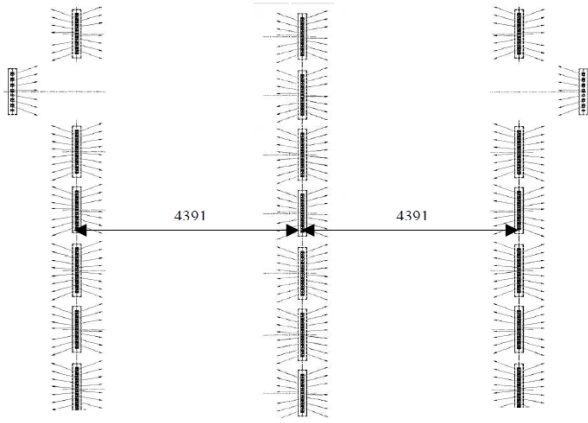


Figure 2: Nozzles of protection air on front and rear wall

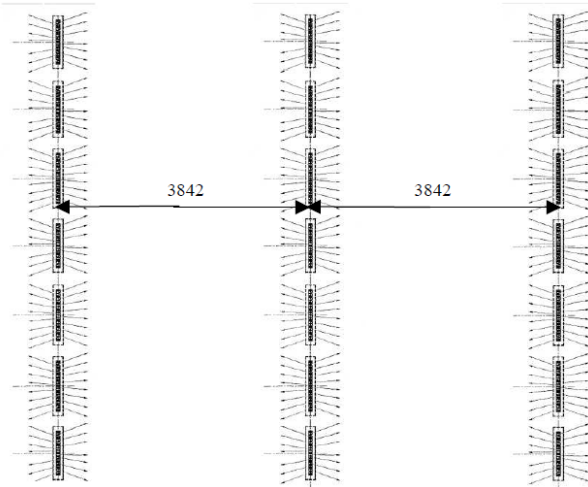


Figure 3: Nozzles of protection air on left and right wall

Advisable in [3] and presented in this article Case B for the functioning of PAS was the basic case for comparative analysis of modeling air distribution between the burners and the OFA (SOFA) nozzles. The Protection Air System (PAS) was combined with 2016 nozzles. There are three columns of air nozzles present on each boiler wall. Seven sets of nozzles are situated in each column. Eight air protection nozzles with outflow on the left side, the right side and inside the boiler are located in each set of protection

nozzles. On the front and rear wall on SOFA level the set of protection nozzles was moved on the left or right side of the wall so that the PAS did not overlap with SOFA nozzles – Fig. 2. In calculations only six set of protected nozzles were taken into account (the set at the highest level was not considered) – Fig. 2, Fig. 3.

#### 4. Numerical model

Table 5: Coal granulation

x	R <sub>x</sub>
<i>μm</i>	%
88	30.6
102	22.0
120	15.4
150	8.3
200	2.24

Table 6: Coal analyses (labour state)

$Q_i^r$	$\frac{kJ}{kg}$	25584
$A^r$	%	12.9
$W_t^r$	%	8.5
$C^r$	%	65.33
$H^r$	%	4.23
$S^r$	%	0.62
$O^r$	%	7.37
$N^r$	%	1.05

Set out in 3 are the turbulence, combustion, radiation and particle treatment described in the sub model and used in the numerical modeling of the boiler. The setup of the parameters of the boiler operating conditions is shown in Table 4 – its input data was entered into Ansys Fluent. Boiler was fired with bituminous coal; see granulation in Table 5 and coal analyses (labour state) in Table 6.

The geometrical model and numerical mesh of the BP 1150 combustion chamber are shown on Fig. 4 and Fig. 5. The module of the numeric mesh for PAS is part and parcel of the boiler model, where burners, OFA and SOFA nozzles and the protection air system operation were

Table 3: Sum models used in simulations [4]

Two phase model	Euler-Lagrange
Turbulence model	k-e
Combustion model	<ul style="list-style-type: none"> <li>– Non-Premixed Combustion</li> <li>– mixture fraction/PDF</li> <li>– in chemical equilibrium</li> <li>– non adiabatic conditions</li> </ul>
for coal particle	
– devolatilization	single – rate model
– combustion	kinetics – diffusion model
Radiation model	P1
spherical shape of coal particle was assumed	
Rosina-Rammlera-Sperlinga distribution was used	

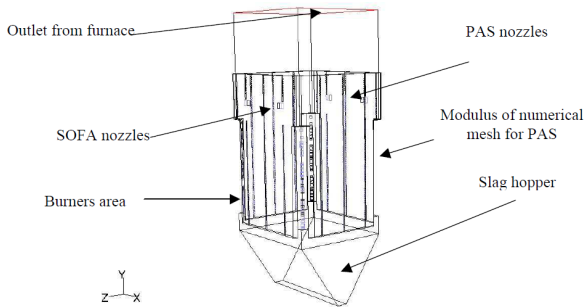


Figure 4: Contour of combustion chamber of BP 1150 boiler

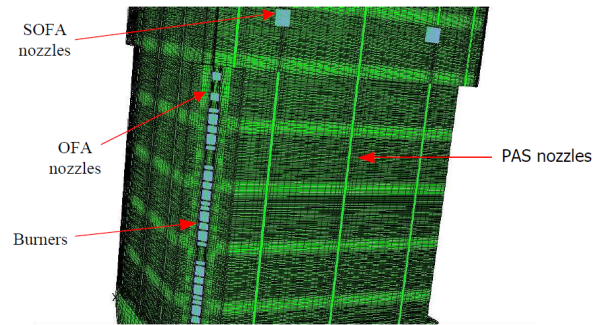


Figure 5: Numerical mesh of combustion chamber and PAS of BP 1150 boiler

modeled. This module was made to improve calculations for the PAS area – Fig. 4.

The modeled boilers contain geometrical elements with a different scale of cells. (PAS nozzles and combustion chamber). Hence, the numerical mesh made in non-conformal technique was used for simulations. In areas with a smaller scale of cells than the furnace (PAS nozzles) a fine mesh was used. In all areas of the furnace a structural mesh was used.

## 5. Numerical results

### 5.1. Results for case worked with PAS marked as B

Fig. 6 and Fig. 7 show the contour of temperature and velocities in three planes located in the section of: fourth row of burners, SOFA nozzles and outlet area .

Distribution of O<sub>2</sub>-CO in the boundary layer of flue gas near the whole water wall of the furnace is shown in Fig. 8 and Fig. 9. The visible lack of oxygen on the rear and front wall of combustion chamber occurred locally – by closing the nozzles in the column of the protection air system near the corners (only the central column worked) the

Table 4: Setting up of parameters of boilers operating conditions

Date	Unit	LF	LR	RR	RF	Sum
Air stream I	$\frac{kg}{s}$					119.96
Mill 1 – bottom	$\frac{kg}{s}$	0.90	0.90	0.90	0.90	3.63
Mill 2	$\frac{kg}{s}$	5.75	5.75	5.75	5.75	23.00
Mill 3	$\frac{kg}{s}$	5.75	5.75	5.75	5.75	23.00
Mill 4	$\frac{kg}{s}$	5.75	5.75	5.75	5.75	23.00
Mill 5 – upper	$\frac{kg}{s}$	5.75	5.75	5.75	5.75	23.00
Coal stream	$\frac{kg}{s}$					35.20
Mill 1 – bottom	$\frac{kg}{s}$	-	-	-	-	0
Mill 2	$\frac{kg}{s}$	2.2	2.2	2.2	2.2	8.8
Mill 3	$\frac{kg}{s}$	2.2	2.2	2.2	2.2	8.8
Mill 4	$\frac{kg}{s}$	2.2	2.2	2.2	2.2	8.8
Mill 5 – upper	$\frac{kg}{s}$	2.2	2.2	2.2	2.2	8.8
Air stream II	$\frac{kg}{s}$	36.8	36.3	36.8	36.3	143.70
Cooling air stream	$\frac{kg}{s}$	6.25	6.25	6.25	6.25	25
Air stream to OFA	$\frac{kg}{s}$	6.14	6.05	6.11	6.08	24.38
Air stream to SOFA	$\frac{kg}{s}$	14.17	14.28	14.14	14.20	56.79
UPO	$\frac{kg}{s}$					28.7
Temperature of air-fuel mixture	$\frac{^{\circ}C}{K}$		101/374			417.56
Temperature of air II	$\frac{^{\circ}C}{K}$		289/562			

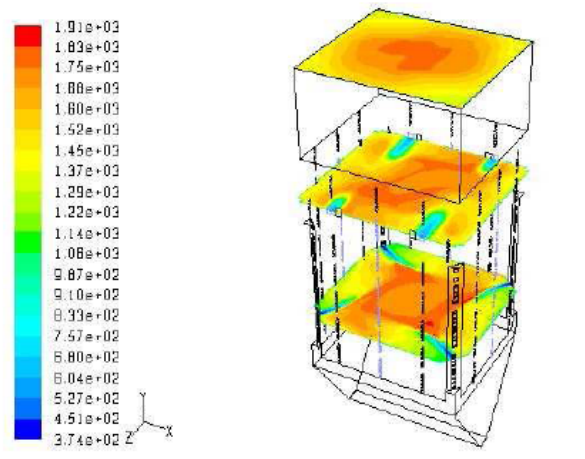


Figure 6: Contour of temperature in three planes

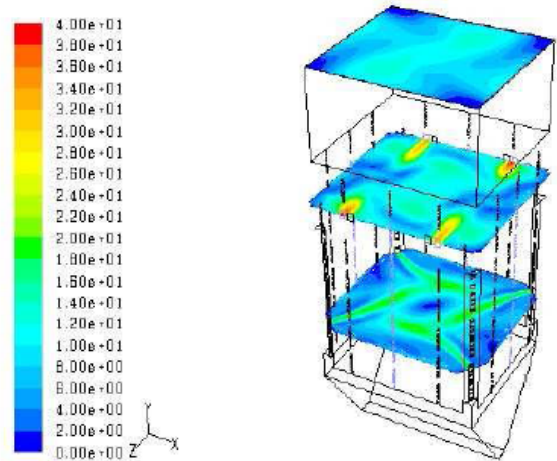


Figure 7: Contour of velocities in three planes

velocities in PAS nozzles increased so that the air from it could overcome the reversed near walls and counteract the circular combustion vortex motion of the boundary layer of flue gas. As the front and rear walls have a bigger horizontal dimension, the effect described above is more visible on the front

and rear walls than on the left and right walls. It could also be observed in Fig. 10 that the velocity of protection air on the outlet from PAS nozzles is about 30 m/s, so it is compatible with the brief preliminary design shown in Table 2. The re-

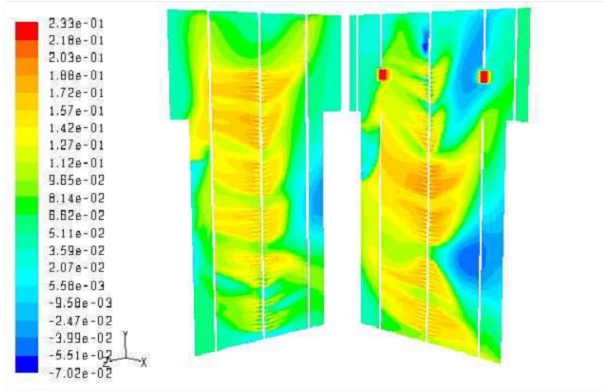


Figure 8: Distribution of O<sub>2</sub>-CO in boundary layer of flue gas near left and rear waterwall

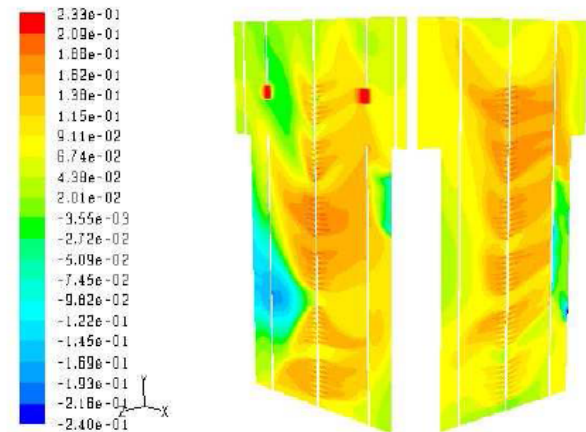


Figure 9: Distribution of O<sub>2</sub>-CO in boundary layer of flue gas near right and front waterwall

versed vortex that occurred in this case vanished due to the motion of protection air – Fig. 11.

## 5.2. Distribution of air between burners and OFA (SOFA) nozzles

Table 7: Varying ratio of secondary air as a proportion to all air in %

	base -B	w1	w2
II	0	-3.75	-7.5
OFA	0	-3.75	+3.75
SOFA	0	0	+3.75

The distribution of primary and secondary air was done so that the ratio of air from PAS was stable at 10% of secondary air. The second criterion was decrease of NO<sub>x</sub> emission – for that purpose the share of secondary air to OFA and SOFA

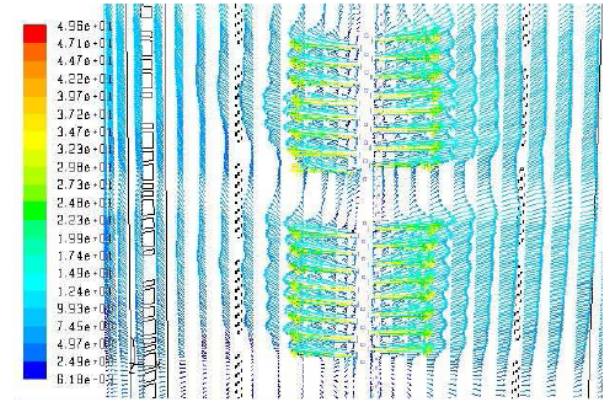


Figure 10: Air's velocity at outlet of PAS nozzles

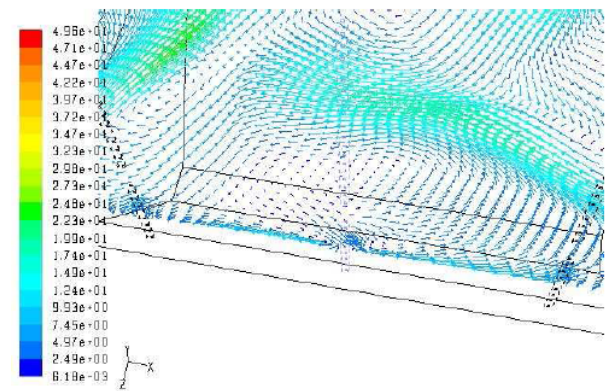


Figure 11: Not big reversed swirl near wall

nozzles was increased at the cost of secondary air from burners. Two cases of air distribution to OFA and SOFA nozzles were modeled – w1 and w2. Case B was the base for making comparisons with Cases w1 and w2. Table 7 shows the varying ratio of secondary air (secondary air from burners, OFA, SOFA) in proportion to all air as a percentage for the modeled cases. For Case B working with PAS also the working of PAS with air distribution to OFA and SOFA nozzles was modeled according to Case w1 and w2.

### 5.2.1. Case B – base

Table 8 presents the distribution of primary and secondary air for base Case B. The ratio of air supplied to burners as secondary air was 51% of secondary air. The velocity of air at the outlet of burner was 43.6  $\frac{m}{s}$ . The ratio of air supplied to OFA nozzles was 9% of secondary air. The velocity of air at the outlet of OFA's nozzles was

Table 8: Distribution of primary and secondary air – base Case

Nozzles	Share of all air		Share of secondary air	Velocity	Stream	
	Primary	Secondary			$\frac{m}{s}$	$\frac{m^3}{h}$
	%		%			
Primary air	25			17.1	266129.7	95.6
Secondary air		38.25	51	43.6	407178.5	146.2
Cooling air		6.75	9	15.5	71855.03	25.8
OFA		6.75	9	36.7	71855.03	25.8
SOFA		15.75	21	27.5	167661.7	60.2
PAS		7.5	10	*	79838.9	28.7
	Sum	75	100		1064519	382.3

\*– velocity for Case B worked with PAS is shown in Table 2

$36.7 \frac{m}{s}$ . The ratio of air supplied to SOFA nozzles was 21% of secondary air. The velocity of air at the outlet of SOFA nozzles was  $27.5 \frac{m}{s}$ .

 Table 11: NO<sub>x</sub> emissions in 6% O<sub>2</sub> flue gas for particular Cases

Case	B	w1	w2
NO <sub>x</sub> $\frac{mg}{m^3}$ (6% O <sub>2</sub> )	492.9	340.9	285.5

### 5.2.2. Case w1

Distribution of primary and secondary air for Case w1 was presented in Table 9. The ratio of air supplied to OFA nozzles was approximately 55% higher than in the base case. The velocity of air at the outlet of OFA nozzles increased from  $36.7$  to  $57 \frac{m}{s}$ .

### 5.2.3. Case w2

Table 10 presents the distribution of primary and secondary air for Case w2. The ratio of air supplied to OFA nozzles was approximately 55% higher than in the base case. The velocity of 10 air at the outlet of OFA nozzles increased from  $36.7$  to  $57 \frac{m}{s}$ . The ratio of air supplied to SOFA nozzles was approximately 23% higher than in the base case. The velocity of air at the outlet of SOFA nozzles increased from  $27.5$  to  $34.1 \frac{m}{s}$ .

### 5.2.4. Results of modelling

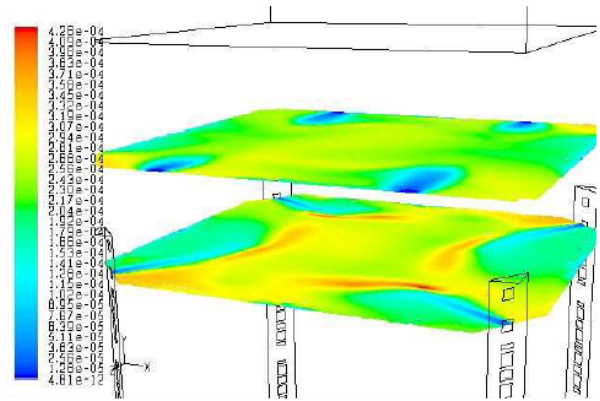

 Figure 12: Mass fraction of NO<sub>x</sub> in OFA1 and SOFA plane – Base case B

Table 9: Distribution of primary and secondary air – Case w1

Nozzles	Share of all air		Share of secondary air	Velocity	Stream	
	Primary	Secondary			$\frac{m}{s}$	$\frac{m^3}{h}$
	%					
Primary air	25		%	17.1	266129.7	95.6
Secondary air		34.5	46	39.3	367259.04	131.9
Cooling air		6.75	9	15.5	71855.03	25.8
OFA		10.5	14	57	111774.5	40.1
SOFA		15.75	21	27.5	167661.7	60.2
PAS		7.5	10	*	79838.9	28.7
	Sum	75	100		1064519	382.3

Bold values changed in relation to the base Case.

Table 10: Distribution of primary and secondary air – Case w1

Nozzles	Share of all air		Share of secondary air	Velocity	Stream	
	Primary	Secondary			$\frac{m}{s}$	$\frac{m^3}{h}$
	%					
Primary air	25		%	17.1	266129.7	95.6
Secondary air		30.75	41	35.3	327339.6	117.6
Cooling air		6.75	9	15.5	71855.03	25.8
OFA		10.5	14	57	111774.5	40.1
SOFA		19.5	26	34.1	207581.2	74.5
PAS		7.5	10	*	79838.9	28.7
	Sum	75	100		1064519	382.3



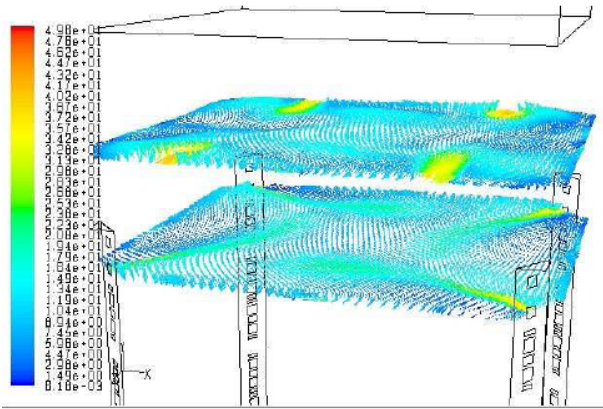


Figure 13: Vectors of velocity in OFA1 and SOFA plane – Base case B

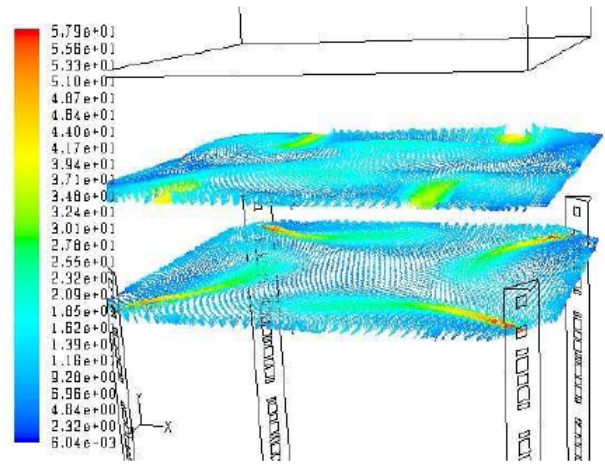


Figure 15: Vectors of velocity in OFA1 and SOFA plane – Case w1

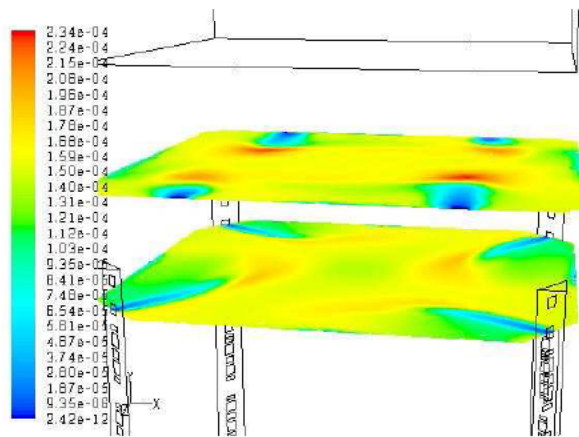


Figure 14: Mass fraction of  $\text{NO}_x$  in OFA1 and SOFA plane – Case w1

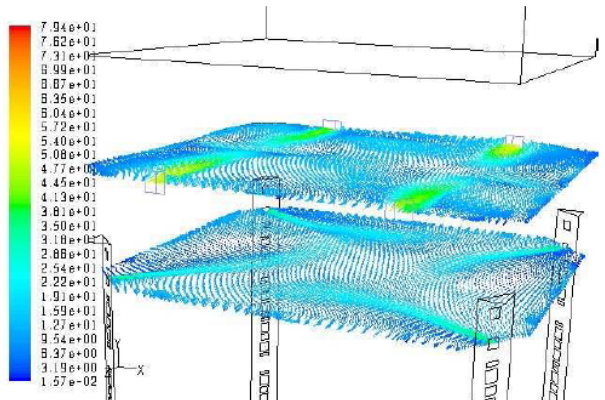


Figure 17: Vectors of velocity in OFA1 and SOFA plane – Case w2

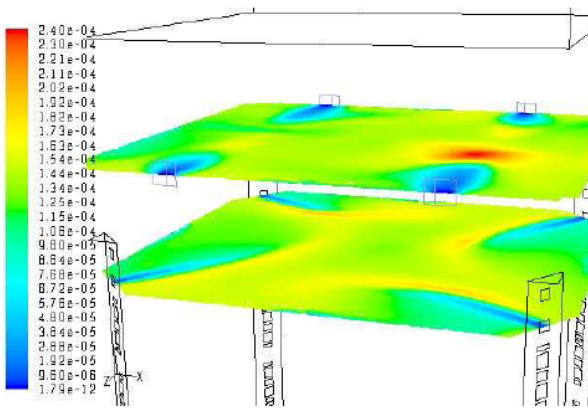


Figure 16: Mass fraction of  $\text{NO}_x$  in OFA1 and SOFA plane – Case w2

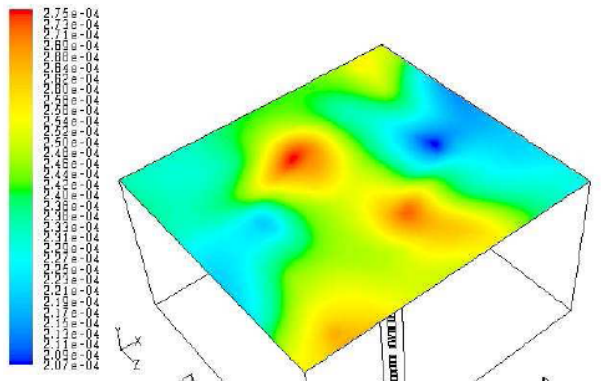


Figure 18: Mass fraction of  $\text{NO}_x$  in outlet plane – Base case B

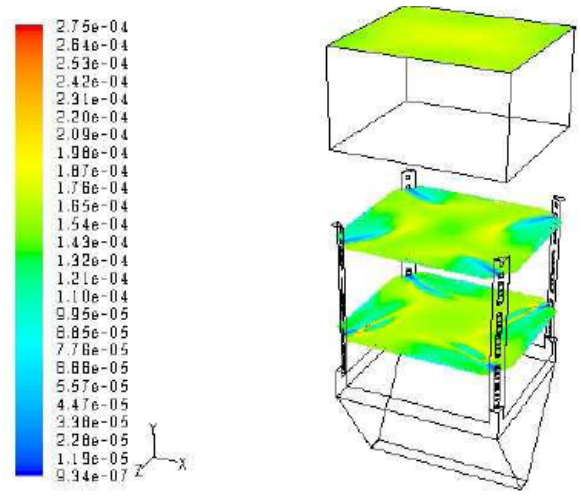
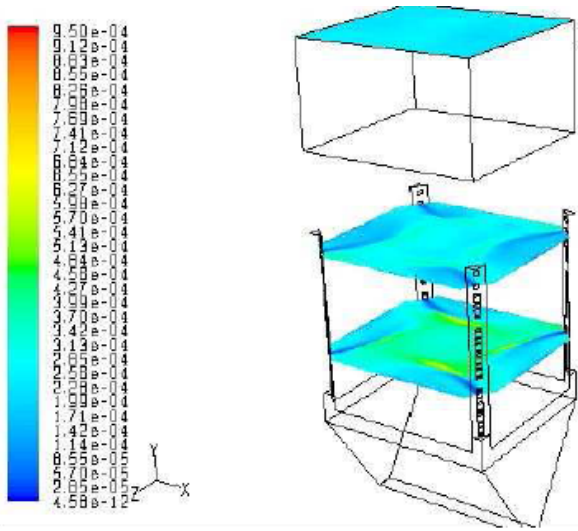


Figure 19: Mass fraction of  $\text{NO}_x$  in burners level four, OFA1 and outlet plane – Base case B

Figure 21: Mass fraction of  $\text{NO}_x$  in burners level four, OFA1 and outlet plane – Case w1

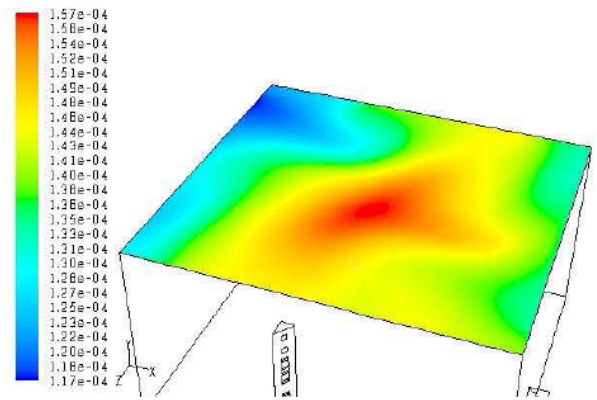
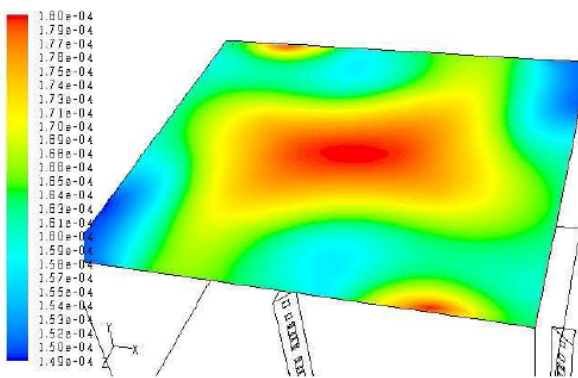


Figure 20: Mass fraction of  $\text{NO}_x$  in outlet plane – Case w1

Figure 22: Mass fraction of  $\text{NO}_x$  in outlet plane – Case w2

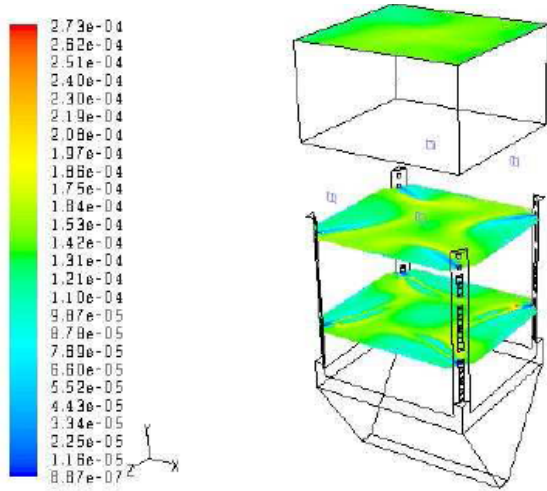


Figure 23: Mass fraction of  $\text{NO}_x$  in burners level four, OFA1 and outlet plane – Case w2

The results of numerical modeling of  $\text{NO}_x$  emissions in 6%  $\text{O}_2$  flue gas for particular cases is shown in Table 11.

In  $\text{NO}_x$  emission calculation the Ansys Fluent  $\text{NO}_x$  model was used. Thermal and Fuel pathways of formation of  $\text{NO}_x$  was used. For Turbulence interaction PDF – a mixture fraction was taken. The partial equilibrium approach was used to determine the concentration of OH and O. The intermediate species selected was HCN/ $\text{NH}_3$ /NO and the char N conversion path selected was NO. Increasing the ratio of air supplied to OFA nozzle by about 55% over the base case caused a Decrease in  $\text{NO}_x$  emission of about 30%, while additionally increasing the ratio of air supplied to SOFA nozzle by about 23% over the base case decreased  $\text{NO}_x$  emission by about 42%. The mass fraction of  $\text{NO}_x$  and vectors of velocity in OFA1 and SOFA plane for the modeled cases is shown in Fig. 12 to Fig. 17. The mass fraction of  $\text{NO}_x$  at outlet, burners level four and OFA1 plane is presented in Fig. 18 to Fig. 23.

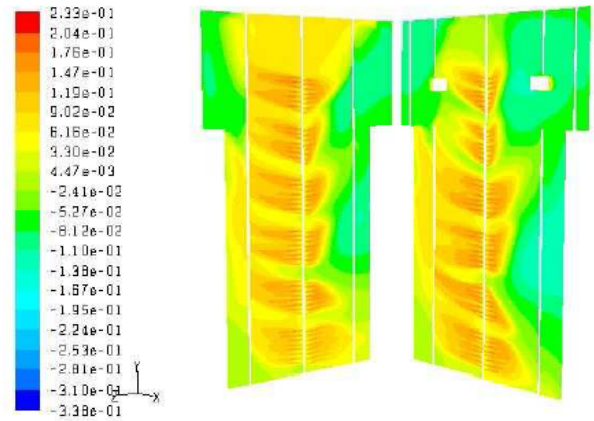


Figure 24: Distribution of  $\text{O}_2$ -CO in boundary layer of flue gas near left and rear waterwall – Case w1

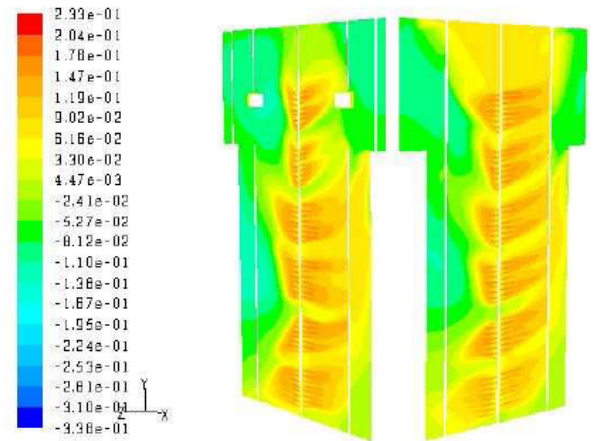


Figure 25: Distribution of  $\text{O}_2$ -CO in boundary layer of flue gas near right and front waterwall – Case w1

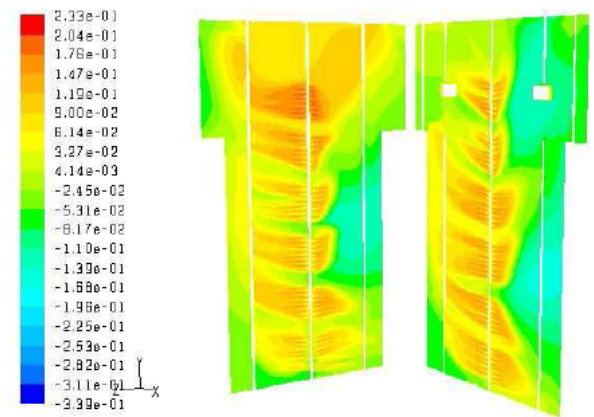


Figure 26: Distribution of  $\text{O}_2$ -CO in boundary layer of flue gas near left and rear waterwall – Case w2

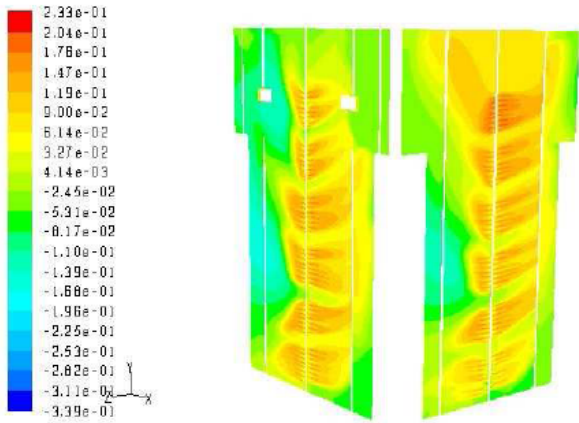


Figure 27: Distribution of O<sub>2</sub>-CO in boundary layer of flue gas near right and front waterwall – Case w2

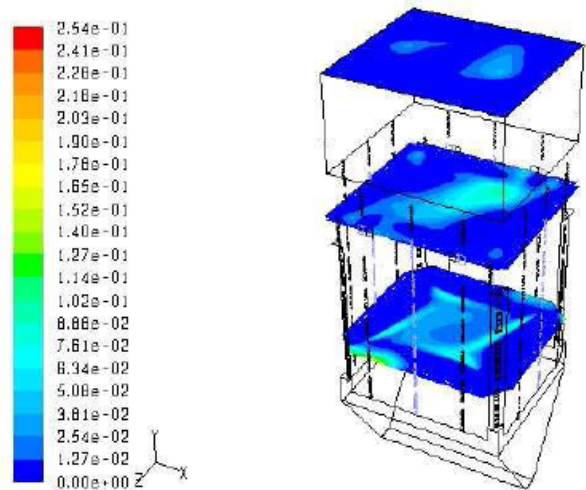


Figure 29: Mass fraction of CO in burners level four, OFA1 and outlet plane – Base case B

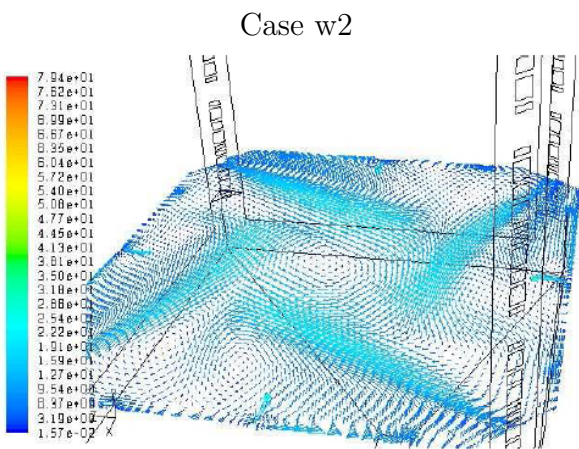
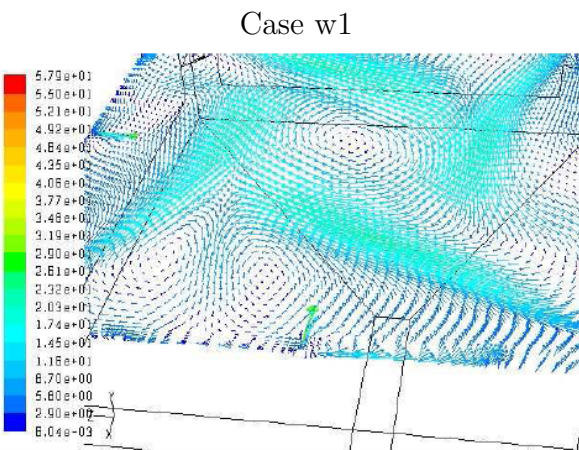


Figure 28: Distribution of O<sub>2</sub>-CO in boundary layer of flue gas near right and front waterwall

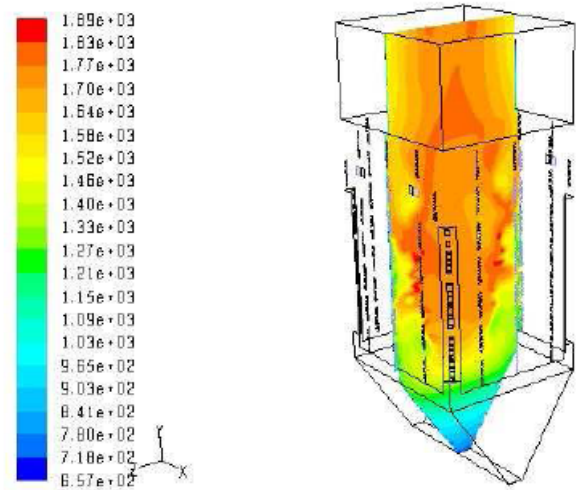


Figure 30: Flue gas temperature along furnace – Base case B

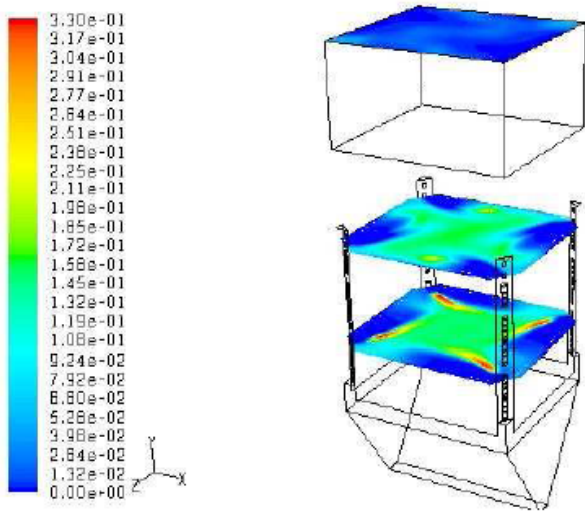


Figure 31: Mass fraction of CO in burners level four, OFA1 and outlet plane – Case w1

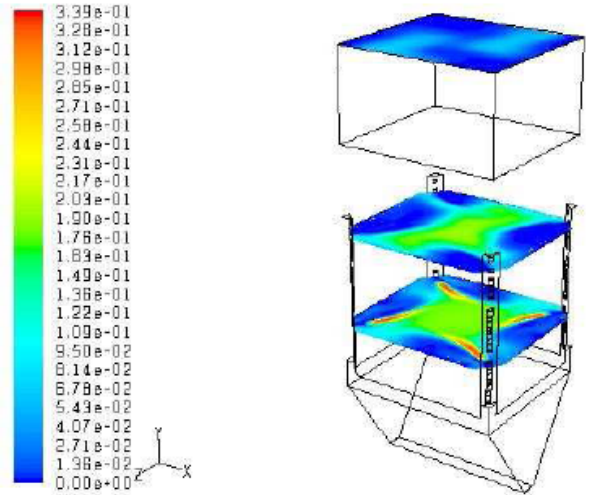


Figure 33: Mass fraction of CO in burners level four, OFA1 and outlet plane – Case w2

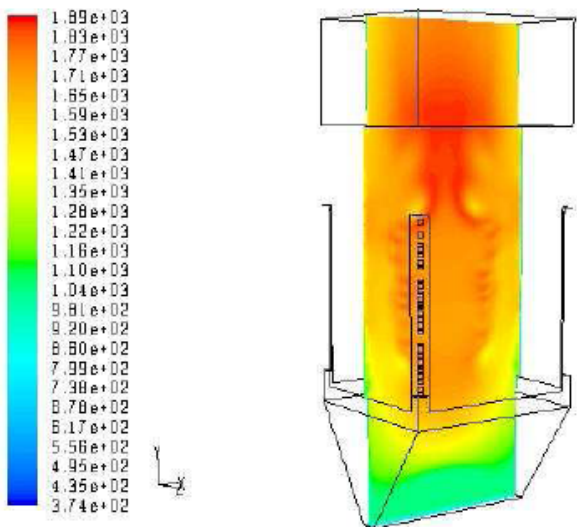


Figure 32: Flue gas temperature along furnace – Case w1

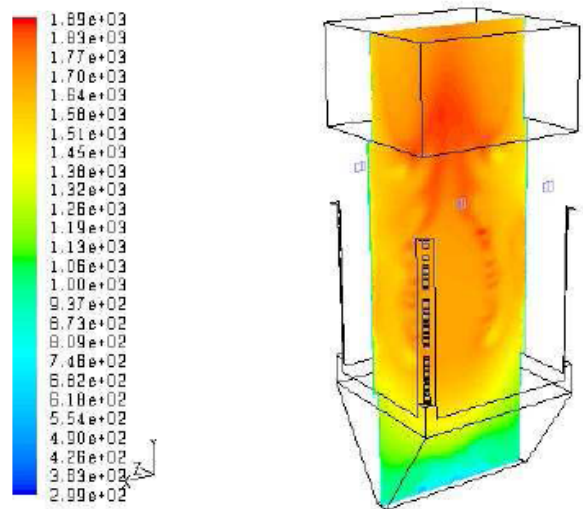


Figure 34: Flue gas temperature along furnace – Case w2

To reduce  $\text{NO}_x$  emissions below  $280 \frac{\text{mg}}{\text{m}^3}$  (6%  $\text{O}_2$ ) staggered air and fuel should be applied. For Cases w1 and w2 the protection air system was modeled. The distribution of  $\text{O}_2$ -CO in the boundary layer of flue gas near the whole water wall in the furnace for Cases w1 and w2 is presented in Fig. 24 to Fig. 27. The visible lack of oxygen on the left wall of the combustion chamber occurred locally and it is connected with reversed nearwalls occurred in this region opposite to the direction of the protection air motion of the

boundary layer of flue gas – Fig. 28. The protection air system works more effectively upon modification of the ratio of secondary air. Combustion was spread out over the length of the combustion chamber and CO concentrates in the region of the circle of the combustion vortex, in contrast to the base case where it occurs near the water wall of the furnace – Fig. 29 to 34.

## 6. Conclusion

The numerical simulation of the combustion chamber of the BP 1150 boiler confirmed that increasing air, after burning, to OFA and SOFA nozzles at the cost of burners secondary air (staggered air concept), efficiently decreases  $\text{NO}_x$  emission and shows  $\text{NO}_x$  concentrations at various levels of the combustion chamber. Increasing the ratio of air supplied to OFA nozzle by approximately 55% over the base case causes a decrease in  $\text{NO}_x$  emission by about 30%, while additionally increasing the ratio of air supplied to SOFA nozzle by approximately 23% over the base case decreases  $\text{NO}_x$  emission about 42%. For Cases w1 and w2 the protection air system was modeled. The distribution of  $\text{O}_2$ -CO in The boundary layer of flue gas near the whole water wall in the furnace for Cases w1 and w2 demonstrated that the protection air system worked better with staggered air. After considerable modification of the ratio of secondary air to OFA and SOFA nozzles combustion was spread out over the length of the combustion chamber and CO concentrated in the region of the circle of the combustion vortex, in contrast to the base case where it was near to the water wall of the furnace. The assumption in the calculation that the ratio of protection air should be 10% of secondary air produces the best results for Cases w1 and w2 of working boilers in terms of working PAS – the best results in air distributions along the water walls caused a decrease in CO concentrations in the boundary layer of flue gas in the combustion chamber of the BP 1150 boiler.

## References

- [1] The Minister of Environment of 20 December 2005 on emission standards for installations [Rozporządzenie Ministra Środowiska z dnia 20 grudnia 2005 r. w sprawie standardów emisyjnych z instalacji].
- [2] Directive 2001/80/ec of the european parliament and of the council of 23 october 2001.
- [3] B. Hernik, R. Litka, Selection of velocity and quantity of secondary air to the burners and nozzles OFA [dobór prędkości i ilości powietrza wtórnego do palników i dysz OFA], Tech. rep., unpublished.
- [4] B. Hernik, Research to reduce the risk of corrosion and erosion of power boilers [badania dla zmniejszenia zagrożenia korozyjno-erozyjnego kotłów energetycznych], Ph.D. thesis, Silesian University of Technology, Gliwice (2009).